

Increasing the Power Density of E-Motors by Innovative Winding Design

Conference Paper**Author(s):**

Stöck, Martin; Lohmeyer, Quentin; Meboldt, Mirko

Publication date:

2015

Permanent link:

<https://doi.org/10.3929/ethz-b-000099028>

Rights / license:

[Creative Commons Attribution-NonCommercial-NoDerivatives 4.0 International](#)

Originally published in:

Procedia CIRP 36, <https://doi.org/10.1016/j.procir.2015.01.078>

CIRP 25th Design Conference Innovative Product Creation

Increasing the power density of e-motors by innovative winding design

Martin Stöck*, Quentin Lohmeyer, Mirko Meboldt

pd/z Product Development Group Zurich, Eidgenössische Technische Hochschule ETH Zürich, Switzerland

* Corresponding author. Tel.: +41 81 758 09 48; fax: +41 (0)81 758 19 99. E-mail address: martin.stoeck@brusa.biz

Abstract

In the future, the sustainable use of renewable energy is becoming more important. About 80% of the total world energy demand is actually derived from fossil fuels. Mobility currently uses over 50% of total global energy. Approaches for the efficient and sustainable energy use are electric and hybrid vehicles. An important component to power these cars is the electric motor. The economic and efficient design of an electric motor requires knowledge of the exact thermal conductivities of all components. A difficult parameter to determine and to improve is the thermal conductivity of the winding. This paper presents measurement results of an innovative motor winding with an improved thermal conductivity.

© 2015 The Authors. Published by Elsevier B.V. This is an open access article under the CC BY-NC-ND license (<http://creativecommons.org/licenses/by-nc-nd/4.0/>).

Peer-review under responsibility of the scientific committee of the CIRP 25th Design Conference Innovative Product Creation

Keywords: Electric motor; power density; thermal conductivity; winding

1 Introduction

A sustainable use of renewable energy is becoming more and more important. About 80% of the total world energy demand is actually covered by fossil fuels [1]. Mobility is currently responsible for more than 50% of the world's energy consumption [2]. Electric and hybrid vehicles are a promising approach for a more efficient and sustainable energy use. In these vehicles, conventional combustion engines are replaced by electric motors. One key challenge of this upcoming industrial application consists in finding novel ways to realize energy efficient electric motors characterized by a high level of power density. The power density is measured by the amount of mechanical output power per motor volume. The main limiting factor to increase the continuous power density is the thermal conductivity of its winding [3]. If an increased thermal conductivity of the winding can be reached, the cooling of the motor is improved and consequently additional power can be produced. Based on a new manufacturing process of winding bars, which allows a higher degree of design freedom [4,5], this paper addresses the research question of how this freedom can be successfully utilized to increase the thermal conductivity of the winding and thus to reach higher power densities of electric motors.

The paper presents two basic design approaches to increase the thermal conductivity of motor windings. Multiple design variants are produced and experimentally evaluated on a test bench built for this purpose. The findings allow a basic understanding of the factors which influence the thermal conductivity. The results also indicate the basic opportunity to increase the power density of electric motors by a smart winding design, and thus to support a more sustainable use of energy.

The paper is structured as follows: Section 2 gives a literature overview regarding thermal conductivity of motor windings and presents published methods to identify the thermal conductivity of defined winding probes. In section 3, the experimental setup to accurately measure the thermal conductivity of winding probes is introduced. Further, a method to minimise the measurement error of the setup is described. Section 4 presents the measurement results. At first, reference probes are measured to check the accuracy of the measurement setup. Then, the results of the winding probes are presented. In section 5 the measurement results are discussed and the factors, which improved the thermal conductivity of the winding, are determined. Section 6 concludes with an overview and an outlook for further research.

2 Literature review

The continuous power density of an electric motor is limited by the thermal consistency of the used materials. Until now, in electric motor design "thermal analysis has received less attention than electromagnetic design. However, in the new century, the topic had started to receive more importance due to market globalization and the requirement for smaller, cheaper, and more efficient electric motors" [6]. Thermal analyses of electric motors are often performed by thermal simulations, which require accurate conductivity values as input. Since the thermal resistance of the winding is dominant compared to all the other thermal resistances, its conductivity is of major interest. A literature research about the thermal conductivity of the winding is summarized in figure 1. It can be seen that the found values spread over a wide range which is not suitable for accurate thermal simulations.

To understand the spreading of these values, the methods used to identify the thermal conductivity of the winding are analysed. Most publications describe a parameter adjustment of a FEM model [6] or an analytic model [7] in order to match the measured temperatures in a motor. All these methods have the disadvantage that for the precise determination of one parameter all the others have to be precisely known. Often these circumstances are not given. Another issue of these methods is that for every variation a new cost intensive motor has to be built. An alternative method is to measure the thermal conductivity in an experiment, but only little research was done in the measurement of the thermal conductivity of winding probes. Simpson et al. [8] for example describes a test setup which can measure the thermal conductivity of cubic winding probes. However, they do not treat the important topic of the measurement accuracy. Therefore, a measurement setup with an optimised measurement error is needed to investigate the thermal conductivity of winding probes with different filling factors and geometry parameters.

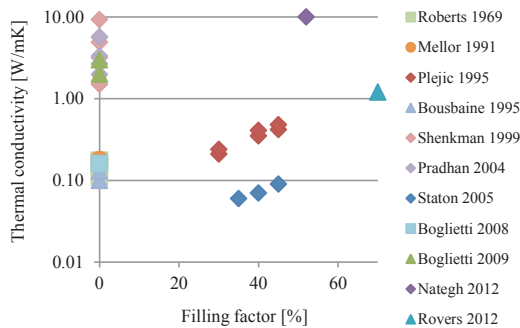


Figure 1: Thermal conductivities of windings of electric motors found in literature (values found without the filling factor information are shown at filling factor zero) [6, 7, 15, 16, 17, 18, 19, 20, 21, 22, 23]

New winding forms like twisted windings were only recently investigated. Van der Geest et al. presented a loss reduction of 60% by replacing parallel windings with twisted windings in an electric motor [9]. This new idea is also described in a recent patent where bars composed of twisted wires are inserted in an electric motor [4]. However, the influence of the twisted wires on the thermal conductivity has not been investigated yet.

To get accurate values for the thermal conductivity of winding probes and to do basic research to understand the influencing factors, a measurement setup is suggested. For the design of a precise measurement setup it is important to analyse and to minimize the measurement error. Using this setup fast and cost-saving measurements of a large amount of winding probes get possible. Further, the difference of the thermal conductivity of twisted- and parallel-wires can be shown experimentally.

3 Measurement of the Thermal conductivity

A Measurements setup, shown in Figure 2, is built to establish a basic knowledge of the windings thermal conductivity. To achieve comparable measurement results of the winding probes, a maximal measurement error of 8 % is required. Increased measurement reliability is achieved by a configuration where all measurements are done redundant. A minimisation of the measurement error is achieved through a geometry optimisation with the help of an analytical model. The assumptions which are made for the simplified analytic model are confirmed by a 3D-FEM simulation.

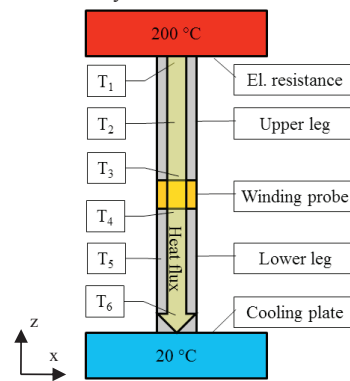


Figure 2: the schematic heat flux in z-direction

The thermal resistance of the winding probe is calculated by dividing the measured temperature drop over the winding probe through the measured heat flux traversing it. With the help of the geometrical parameter of the winding probe (height of the probe: d), the thermal conductivity can be determined [10]. To measure the described values, the winding probe is clamped between two metal legs. A heat flow is imposed on the top of the upper leg by electric resistances. This heat flow goes from the upper leg through the winding probe in the lower leg which is cooled by a cooling plate on the bottom side. The heat flux is calculated by the temperature drop in the two legs $T_1 - T_3$ which is measured by two thermocouples separated at a distance d_{13} . The temperature drop over the winding probe $T_3 - T_4$ is measured by two thermocouples located near the probe in each leg. To compensate the temperature drop between the probe surfaces to the measuring point, a linear extrapolation of the three measured temperatures in the leg is done up to the probe surface. Since three measurements are performed in each leg, a redundancy for the linear interpolation is guaranteed. The redundancy of the heat flux is provided by measuring the heat flux twice, in the upper and in the lower leg. To finally calculate the thermal conductivity, an analytic model is done.

For this analytic model, three assumptions are made: 1) The imposed heat flux and the temperature are considered as uniformly distributed over the upper surface of the leg. This assumption seems justified because the electric resistances are mounted on an aluminium plate with a high thermal conductivity. 2) The heat flow in the leg is considered as unidirectional in z direction. This approximation appears also correct because the area surrounding the legs is isolated with mineral wool. 3) The holes in the legs where the thermocouples are placed do not significantly influence the measurements. Since the holes have a diameter of only 0.5 mm, this assumption seems also reasonable. These three assumptions will be verified at the end of this chapter. The analytic model is developed on the base of these assumptions. To simplify the explanation, the following equation determines the thermal conductivity of the probe λ_{probe} considering a non-redundant measurement:

$$\lambda_{probe} = \lambda_{Leg} \frac{d}{d_{13}} \frac{T_1 - T_3}{T_3 - T_4} \quad (1)$$

To quantify the measurement uncertainty $u(\lambda_{probe})$ the propagation of uncertainty (2) is applied to each parameter x_i of (1). The calculated measurement uncertainties of each parameter are shown in Table 1.

$$u(\lambda_{probe})^2 = \sum_i \left(\frac{d\lambda_{probe}}{dx_i} u(x_i) \right)^2 \quad (2)$$

By applying this formula, the influence of all parameters to the measurement uncertainty can be calculated [11]. In order to minimize the total uncertainty, the influence of every single parameter has to be minimized to a common level. It emerged that the uncertainty of the thermal conductivity of the metal legs λ_{Leg} and the uncertainty of the probe height have a significant impact on the total measurement uncertainty. Therefore, these two parameters are investigated further. The thermal conductivity of common steel is usually not very precisely reported by the manufacturers and is strongly dependent on the temperature [12]. A material which is suitable for the application is the Armco-Iron which is chosen by R. W. Powell as the „thermal-conductivity standard“ [13]. To measure the height of the probe, two pins are placed on the sides of the legs. These pins allow a precise measurement of the probe height by using a micrometre. Thank to these improvements, the sensitivity coefficient of all parameters is reduced to a common level (see Table 1).

Table 1: Calculated measurement uncertainty

Parameter	Nominal Value, x_i	Uncertainty of each parameter, $u(x_i)$	Sensitivity coefficient $d\lambda_{probe}/dx_i * u(x_i)$ [W/(mK)]
λ_{leg}	65 W/(mK)	1.3 W/(mK)	0.0100
d	3.45 mm	0.03 mm	0.0019
d_{13}	40 mm	0.7 mm	0.0077
T_1	180 °C	0.65 °C	0.0040
T_3	128.74 °C	0.65 °C	0.0144
T_4	71.26 °C	0.65 °C	0.0032

For the defined probe geometry, excluding the height of the legs (d_{13}), all the measurement uncertainties are given by the datasheet of the chosen components or the manufacturing process. It is of major importance to fix this parameter correctly, since with too long or too short legs the measurement uncertainty increases. Too long legs cause a high temperature drop ($T_1 - T_3$) in the leg. So the heat flux in the leg can be calculated precisely, but the temperature drop over the probe ($T_3 - T_4$) gets imprecise. With too short legs, the partition of the temperature drop becomes the opposite, but the measurement error remains high. Therefore, an optimum has to be found where the heat flux and the temperature drop over the probe can be determined precisely. In order to minimize the measurement uncertainty, the influence of the leg length on the error was calculated by (2) for several thermal conductivities at different leg lengths (see Figure 3). Since the thermal conductivity of the probes is at the beginning not known, thermal conductivities between 1 W/mK and 20 W/mK are supposed. For a uniform weighting of the thermal conductivities, the mean measurement error is calculated. The optimal leg length is found to be around 40 mm. This length is chosen as leg length of the setup.

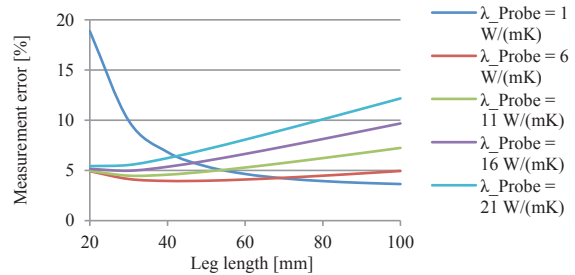


Figure 3: Measurement error in function of the leg length

To verify these results, a thermal FEM-simulation is performed. With this simulation it can be shown that the three made assumptions are correct (max. error of assumptions 1%). Further, the calculated values of the analytic model are compared with the thermal FEM-simulations. Since they are in good agreement (max. error between model and simulation: 2%), the analytic model is found to be applicable.

4 Results of the Measurements

To confirm the precision of the test setup, the calculated measurement uncertainties are verified with the help of reference probes.

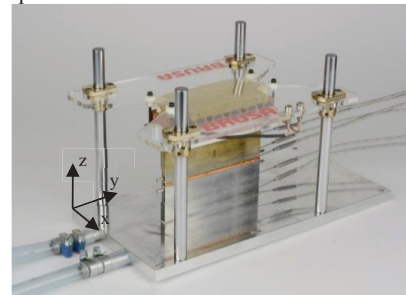


Figure 4: Measurement setup

During the measurements, the cooling and the heat source are switched on. The temperatures in the legs start to rise and stabilise on a higher value (see Figure 5). For each of these values the thermal conductivity can be calculated (see Figure 6), but since the thermal conductivity is a constant value, only measurements at steady state condition make sense.

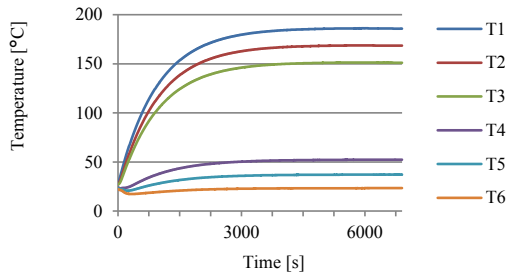


Figure 5: Temperature characteristic of a typical measurement

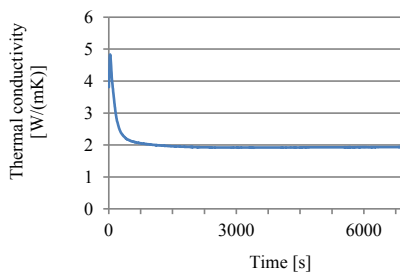


Figure 6: Correspondent calculated thermal conductivity of Fig. 5

With the help of three reference probes, the calculated measurement error of the previous chapter can be verified. The measured values are compared with the values found in literature [14]. As shown in Table 2, the errors between the measurement and the values found in the literature are smaller than the calculated maximal measurement error. This proves that the analytic model to calculate the measurement uncertainty is applicable to the built measurement setup.

Table 2: Comparison of measurement uncertainty and measurement error

Probe	Literature value [W/mK]	Measurement value [W/mK]	Measurement uncertainty [%]	Measurement error [%]
S235JR	54	50.9	± 13.7 %	- 5.6%
PTFE 0.3	0.24	0.215	± 10.7 %	- 10.4 %
PTFE 0.5	0.24	0.246	± 6.9 %	+ 2.5 %

To improve the thermal conductivity of the winding, several probes with different configurations are measured. All measurements are done with the same wire diameter and the same probe geometry. To investigate the dependence of the filling factor of parallel windings, the number of wires in the same cross section is varied (blue curve in Figure 7). To examine the new suggested winding type, a 360° twisted wire bundle (red curve in Figure 7) is compared to parallel windings.

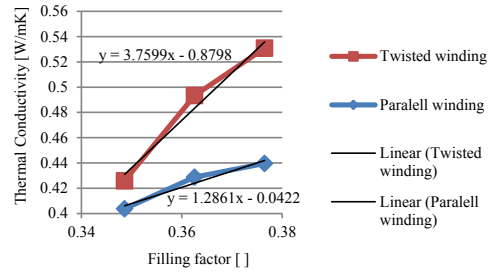


Figure 7: Dependency of the thermal conductivity on the filling factor of different probe types

5 Discussion

An important parameter to increase the continuous power density of electric motors is the thermal conductivity of the winding. To investigate the influence of different winding configurations on their thermal conductivity, a test setup is constructed and validated. With this test setup, the influence of higher filling factors and twisted windings on the thermal conductivity of the winding is investigated.

For parallel windings, the thermal conductivity rises with the filling factor. This effect can be explained by the increased copper content in the cross-section. Since copper has a higher thermal conductivity compared to epoxy and air, a higher total thermal conductivity of the winding probe is achieved by increasing the amount of copper in the probe.

For the twisted winding and the normal winding (parallel winding), the thermal conductivity is investigated in function of the filling factor. Further, two trend-curves are plotted and compared to each other. It can be seen that the twisted winding generally has a higher thermal conductivity. Moreover, the increase of the thermal conductivity with the filling factor is more important for the twisted version than for the parallel version. To explain the higher thermal conductivity of the twisted winding, a 2D model is not sufficient any more, and a 3D model has to be applied. In a twisted wire some conductors touch both, the top and the bottom side of the probe (see Figure 8). Since copper is a good thermal conductor, heat is transferred inside the wire from the top to the bottom. Thermal flow along the wire itself involves a longer path compared to the thermal flow along the cross section of the probe, but along the wire the thermal conductivity is much higher than along the cross-section. Because of the much higher thermal conductivity of the copper (inside the wire) than the epoxy-cooper mixture (cross section), the thermal conductivity along the wire has a positive influence on the global thermal conductivity of the probe. The higher values of the twisted winding can be explained by this effect (shift of the curve). The higher slope can be explained by the same effect which gets more and more dominant when more wires are involved.



Figure 8: Schematic representation of a twisted wire inside a twisted winding probe

As shown in Figure 7, a trend line is added to the parallel and the twisted winding curves. Since the initial idea suggested the utilization of compressed litz wires, it was estimated that the compression could increase the filling factor of the winding up to 80%. For this increased filling factor, the thermal conductivity was extrapolated by the two curves. It can be seen that the twisted version has a 20% to 30% higher thermal conductivity compared to the parallel one at the same filling factor. Comparing the conventional winding technology, where the filling factor is limited by the production process to 45%, to the compressed and twisted winding, an increase of the thermal conductivity of 215% is estimated. Because of these promising results, the effect of the compression on the thermal conductivity of the winding probes has to be investigated further. Nevertheless, the significant increase of the thermal conductivity coupled with the initially mentioned lower losses of a twisted winding is a promising result for the future electric motor development.

It can be shown that the suggested twisted winding has an increased thermal conductivity because the thermal flux is conducted more inside the wire itself than across the wire insulation whose thermal conductivity is low. In addition, a higher filling factor leads to a higher thermal conductivity because it involves more copper in the cross-section which has a higher thermal conductivity than the insulation in between. With the newly suggested winding-type, the insertion of bars with a higher filling factor and twisted wires gets possible. These bars can be composed of compressed twisted wires. Through the utilization of these bars, a significantly increased thermal conductivity is expected. With the higher filling factor the copper losses and therefore the heat generations in the motor can be minimized. Thank to these two effects, a significant increase of the continuous power density of electric motors is expected.

6 Conclusion and Outlook

This paper presents a solution to improve the power density of electric motors used in electric or hybrid cars. Electricity produced by renewable energy sources is one alternative solution for future sustainable mobility. By increasing the power density, a reduced amount of raw materials is required and consequently electric motors get more cost efficient. To achieve higher power densities, a new winding type is suggested. Contrary to actual distributive windings, a fully automatic production process gets possible since winding bars can be inserted in the stator slots automatically. With these bars, the freedom of designing the winding is increased. This offers new possibilities to increase the power density of electric motors. One key factor to increase the power density is to improve the thermal conductivity of the winding. Pre-manufactured winding bars significantly increase the winding design freedom, since the production process allows an unrestricted placement of the single conductors which is not possible with the conventional approach. In this paper, the influence on the thermal conductivity of one promising bar design, namely the use of twisted wires, is investigated.

The values for the thermal conductivity of the motor winding found in literature are non-consistent and no values are found for twisted windings, therefore a test setup to measure the thermal conductivity of winding probes is constructed. To reach a high accuracy, the measurement uncertainty of the

setup is optimised. With this test setup reference probes are measured to guarantee correct results. Further, first measurements with several different winding probes are conducted. The influence of the filling factor of the winding (copper percentage in the cross-section) and a twist in the winding are investigated through measurements. The results for parallel windings with an increased filling factor show an increased thermal conductivity. In addition, a further increase of the thermal conductivity is observed for the twisted winding. The effect for the parallel winding can be explained by a 2D-Model where the total thermal conductivity is composed by several singles conductivities. Since there is more copper in the cross-section and cooper has a higher thermal conductivity than the insulation, a higher total thermal conductivity of the winding results. For the twisted wires the effect is explained by a 3D-model: each single wire has, in the case of twisted wires, the possibility to conduct the heat along each wire. Since some wires touch the upper and the lower side of the winding, an increased thermal conductivity is obtained.

The influence of the filling factor and a twist in the winding can be experimentally shown. Further improvements are expected by increasing the filling factor. More experiments with higher filling factors needs to be conducted. Finally, it can be seen that by applying the proposed twisted winding bars with a higher filling factors, the cooling of the electric motor is improved. Therefore, a higher power density of the motor is achieved. With this new technology a further step towards an affordable solution for sustainable mobility is done.

Acknowledgments

The authors would like to thank the company BRUSA Elektronik AG for supporting research on this topic.

References

- [1] Helen Lindblom et al. (2010): Energy in Sweden facts and figures. The Swedish Energy Agency.
- [2] John Conti et al. (2013): International energy outlook 2013. U.S. Energy Information Administration.
- [3] Boglietti, A.; Cavagnino, A.; Staton, D. A. (2004): TEFC induction motors thermal models: a parameter sensitivity analysis. In: Industry applications conference, 2004. 39th IAS annual meeting., Bd. 4, S. 2469–2476 vol.4.
- [4] Mathoy Arno, Stoeck Martin: Stator. Publication Nr: WO2013190514 (A1) - STATOR.
- [5] Stöck Martin, Lüchinger Philipp Meboldt Mirko: Increase of the power-density in electrical machines by innovative solutions: 24 – 26 June 2014, Hybrid Expo 2014, Stuttgart.
- [6] Boglietti, A.; Cavagnino, A.; Staton, D.; Shanel, Martin; Mueller, M.; Mejuto, C. (2009): Evolution and modern approaches for thermal analysis of electrical machines. In: Industrial Electronics, IEEE Transactions on 56 (3), S. 871–882.
- [7] Boglietti, A.; Cavagnino, A.; Staton, D. (2008): Determination of critical parameters in electrical machine thermal models. In: Industry Applications, IEEE Transactions on 44 (4), S. 1150–1159.
- [8] Simpson, N.; Wrobel, R.; Mellor, P. H. (2013): Estimation of Equivalent Thermal Parameters of Impregnated Electrical Windings. In: Industry Applications, IEEE Transactions on 49 (6), S. 2505–2515.
- [9] van der Geest, M.; Polinder, H.; Ferreira, J. A.; Zeilstra, D. (2014): Current Sharing Analysis of Parallel Strands in Low-Voltage High-Speed Machines. In: Industrial Electronics, IEEE Transactions on 61 (6), S. 3064–3070.

- [10] Bergman, Theodore L. (2011): Fundamentals of heat and mass transfer. 7. Aufl. Hoboken, NJ: Wiley.
- [11] Deutsches Institut für Normung (1996): Evaluation of measurements of a single measurand, measurement. 1996. Aufl. Berlin: Beuth (Deutsche Norm, 1319,3).
- [12] Peet, M. J.; Hasan, H. S.; Bhadeshia, H. K. D. H. (2011): Prediction of thermal conductivity of steel. In: International Journal of Heat and Mass Transfer 54 (11–12), S. 2602–2608.
- [13] Powell, R. W. (1962): 42 - Armco Iron as a Thermal Conductivity Standard. In: JOSEPH F. MASI und DONALD H. TSAI (Hg.): Progress in International Research on Thermodynamic and Transport Properties: Academic Press, S. 454–465.
- [14] VDI e. V. (2013): VDI-Wärmeatlas. Berlin Heidelberg: Springer Berlin Heidelberg (VDI-Buch).
- [15] Bousbaine, A.; McCormick, M.; Low, W. F. (1995): In-situ determination of thermal coefficients for electrical machines. In: Energy Conversion, IEEE Transactions on 10 (3), S. 385–391.
- [16] Mellor, P. H.; Roberts, D.; Turner, D. R. (1991): Lumped parameter thermal model for electrical machines of TEFC design. In: Electric Power Applications, IEE Proceedings B 138 (5), S. 205–218.
- [17] Nategh, S.; Wallmark, O.; Leksell, M.; Shuang Zhao (2012): Thermal Analysis of a PMSRM Using Partial FEA and Lumped Parameter Modeling. In: Energy Conversion, IEEE Transactions on 27 (2), S. 477–488.
- [18] Plejčić, Matjaž; Goričan, Viktor; Hribernik, Božidar (1995): FEM Thermal modeling of an induction motor. In: André Nicolet und R. Belmans (Hg.): Electric and magnetic fields: Springer US, S. 155-158.
- [19] Pradhan, M. K.; Ramu, T. S. (2004): Estimation of the hottest spot temperature (HST) in power transformers considering thermal inhomogeneity of the windings. In: Power Delivery, IEEE Transactions on 19 (4), S. 1704–1712.
- [20] Rovers, J. M. M.; Stöck, M.; Jansen, J. W.; van Lierop, C. M. M.; Lomonova, E. A.; Perriard, Y. (2013): Real-time 3D thermal modeling of a magnetically levitated planar actuator. In: Special Issue on Linear Drives 23 (2), S. 240–246.
- [21] Shenkman, A.; Chertkov, M. (1999): Heat conditions of a three-phase induction motor by a one-phase supply. In: Electric Power Applications, IEE Proceedings - 146 (4), S. 361–367.
- [22] Staton, D.; Boglietti, A.; Cavagnino, A. (2005): Solving the more difficult aspects of electric motor thermal analysis in small and medium size industrial induction motors. In: Energy Conversion, IEEE Transactions on 20 (3), S. 620–628.
- [23] T. J. Roberts (1969): Determination of the thermal constants of the heat flow equations of electrical machines. College of Engineering Technology, Eastlands, Rugby. Department of Electrical Engineering.